

Journal of Materials Chemistry A

Accepted Manuscript



This is an *Accepted Manuscript*, which has been through the Royal Society of Chemistry peer review process and has been accepted for publication.

Accepted Manuscripts are published online shortly after acceptance, before technical editing, formatting and proof reading. Using this free service, authors can make their results available to the community, in citable form, before we publish the edited article. We will replace this *Accepted Manuscript* with the edited and formatted *Advance Article* as soon as it is available.

You can find more information about *Accepted Manuscripts* in the [Information for Authors](#).

Please note that technical editing may introduce minor changes to the text and/or graphics, which may alter content. The journal's standard [Terms & Conditions](#) and the [Ethical guidelines](#) still apply. In no event shall the Royal Society of Chemistry be held responsible for any errors or omissions in this *Accepted Manuscript* or any consequences arising from the use of any information it contains.

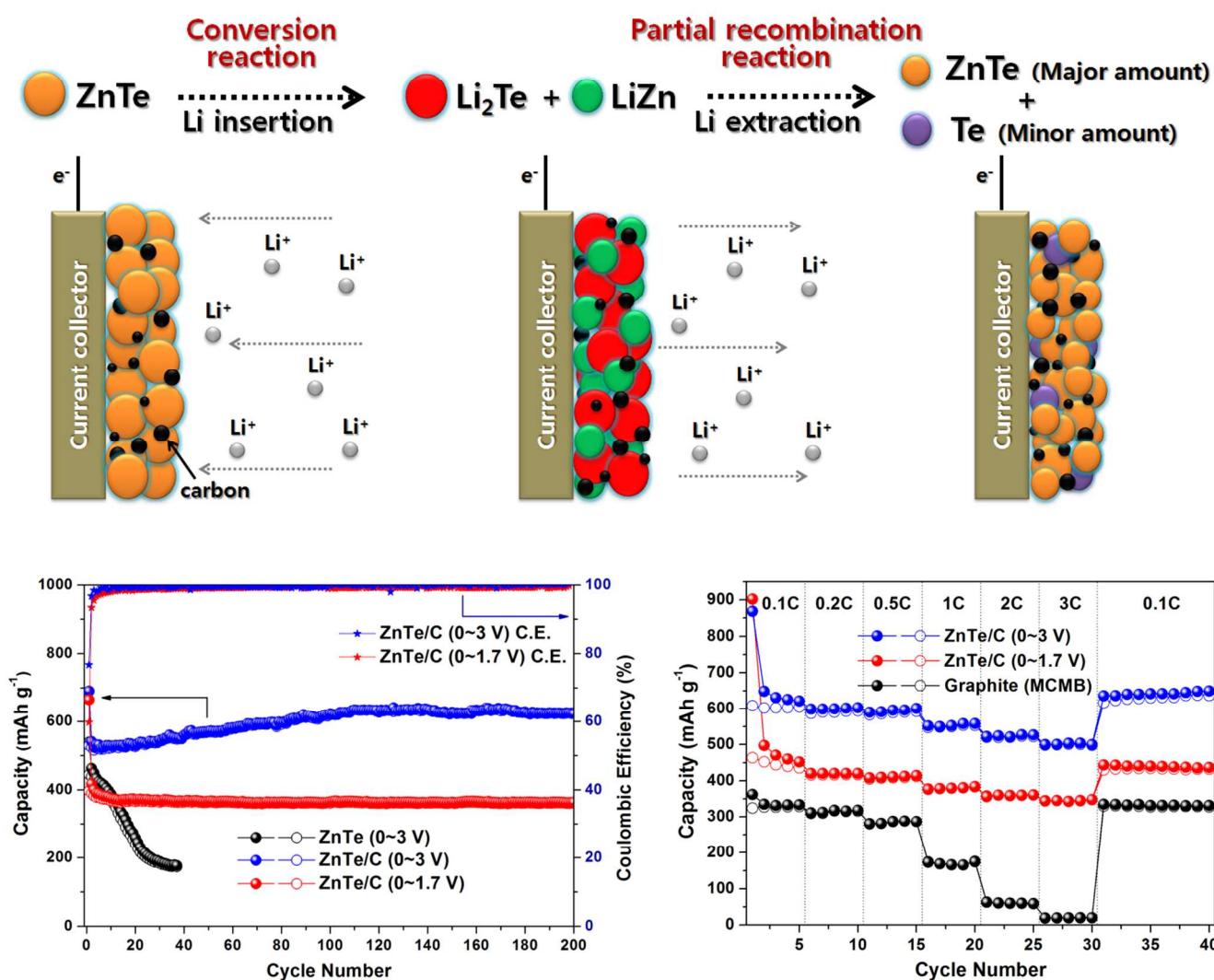
Graphical Abstract

ZnTe and ZnTe/C nanocomposite: A new electrode material for high-performance rechargeable Li-ion batteries

Jeong-Uk Seo & Cheol-Min Park*

ZnTe and a nanostructured ZnTe/C composite were prepared by a simple solid-state synthetic route and their potential as electrode materials for rechargeable Li-ion batteries was investigated.

TOC figure



ZnTe and ZnTe/C Nanocomposite: A New Electrode Material for High-Performance Rechargeable Li-ion Batteries

Cite this: DOI: 10.1039/x0xx00000x

Received 00th January 2012,
Accepted 00th January 2012

DOI: 10.1039/x0xx00000x

www.rsc.org/

Jeong-Uk Seo^a and Cheol-Min Park^{*ab}

Zinc telluride (ZnTe) and a nanostructured ZnTe/C composite were prepared by a simple solid-state synthetic route and their potential as electrode materials for rechargeable Li-ion batteries was investigated. The electrochemical conversion/partial recombination reactions between ZnTe and Li were determined using *ex situ* X-ray diffraction and extended X-ray absorption fine structure analysis. X-ray diffraction and high-resolution transmission electron microscopy confirmed that the ZnTe/C nanocomposite consisted of ZnTe nanocrystallites that were uniformly distributed within an amorphous carbon matrix. The nanostructured ZnTe/C composite electrode exhibited excellent electrochemical properties with a high capacity (1st charge: 530 mAh g⁻¹), cycling durability (over 200 cycles), and fast rate capability (1C: ca. 550 mAh g⁻¹, 3C: ca. 504 mAh g⁻¹).

Introduction

Currently, rechargeable Li-ion batteries are used as a representative rechargeable battery system thanks to their high energy density, slow self-discharge, and lack of memory effect. Graphite is typically used as the anode material in rechargeable Li-ion batteries because of its interesting intercalation behavior, which is associated with the formation of the LiC₆ intercalation compound. However, despite this advantage, the electrochemical performance of graphite anodes is limited as they have a low theoretical capacity (372 mAh g⁻¹ or ca. 840 mAh cm⁻³) and poor rate capability.¹⁻³ Therefore, new alternative anode materials with better electrochemical performances, including higher capacities and faster rate capabilities are highly pursued.¹⁻¹⁰

Although Li metal anode is considered as a promising anode thanks to its high theoretical capacity (3860 mAh g⁻¹), its commercial use has been hindered by various drawbacks.³⁻⁶ Therefore, Li-alloy-based elements such as Li-Sn, Li-Si, Li-Ge, Li-P, and Li-Sb have been proposed as possible anodes for Li-ion batteries because they reversibly react with large ratios of Li.¹³⁻³¹ However, despite their high capacities, these alloys suffer from large volume changes that occur during Li insertion/extraction and result in poor cycling behavior.^{1-3,7-13} To overcome this problem, nanostructured or nanocomposite materials have been suggested.³²⁻³⁵ These materials could provide stable cycling behavior through their accommodation of the strain generated during cycling and enhanced Li storage kinetics because of their larger surface areas, shorter diffusion lengths, and faster diffusion rates.

Among the many Li-alloy-based elements available, Zn-based materials have been suggested as alternative anodes for rechargeable Li-ion batteries because of their high theoretical capacity of ca. 410 mAh g⁻¹ (ca. 2927 mAh cm⁻³) and the ability of Zn to form various Zn-M binary compounds (M = P, Sb, Se, etc.).³⁶⁻⁴¹ Additionally, Zn is an abundant, cheap, and environmentally friendly element. Although Zn-based anodes have been observed to exhibit high capacities, they suffer from poor cycling behavior due to LiZn formation.⁴² Tellurium, a group 16 element, can alloy with Li forming Li₂Te, which has a theoretical capacity of ca. 420 mAh g⁻¹ (ca. 2621 mAh cm⁻³). However, its application to rechargeable Li-ion batteries has not been reported. Considering the electrochemical activity of Zn and Te with Li, they have high potentials as electrode materials for rechargeable Li-ion batteries.

Zinc telluride (ZnTe), a compound of Zn and Te, is an intrinsic semiconducting material, with a band gap of approximately 2.26 eV, commonly used in optoelectronics and is important in the development of various semiconductor devices such as blue LEDs, solar cells, laser diodes, and microwave generators.⁴³⁻⁴⁵ Additionally, the density of ZnTe (6.34 g cm⁻³) is much higher than those of ZnO (5.61 g cm⁻³), ZnS (4.09 g cm⁻³), and ZnSe (5.27 g cm⁻³). The high density of ZnTe results in high volumetric capacity when it is applied to Li-ion battery. Although various applications of ZnTe have been reported, to the best of our knowledge, it has not been tested for its application in rechargeable Li-ion batteries.

In this study, to overcome the problems faced when Zn or Te is used independently as an electrode material, ZnTe and a nanostructured composite (ZnTe/C) were prepared by high energy mechanical milling (HEMM) and tested for their

suitability as electrode materials in rechargeable Li-ion batteries. Furthermore, the reaction mechanism of ZnTe with Li was thoroughly investigated on the basis of ex situ X-ray diffraction (XRD), extended X-ray absorption fine structure (EXAFS) analysis, and the examination of a differential capacity plot (DCP) and cyclic voltammogram (CV).

Experimental

Samples Preparation: ZnTe was synthesized using Zn (Kojundo, 99.9%, average size ca. 100 μm) and Te (Aldrich, 99.98%, average size ca. 50 μm) powders by high energy mechanical milling (HEMM, Spex-8000) at ambient temperature and pressure as follows: Stoichiometric amounts of Zn and Te powders were placed into a 80 cm^3 hardened steel vial with stainless steel balls (diameter: 3/8 in. and 3/16 in.) at a ball-to-powder ratio of 20:1. The HEMM process was carried out under an Ar atmosphere for 6 h. The same HEMM technique was used to obtain a ZnTe/C nanocomposite by milling mixtures of ZnTe and carbon (Super P, Timcal) powders. Preliminary electrochemical tests revealed that, in terms of the electrochemical performance such as initial capacity, initial coulombic efficiency, and cycle performance, the optimum amounts of ZnTe and C were 60 and 40 wt.%, respectively.

Materials Characterization: ZnTe and the ZnTe/C nanostructured composite were characterized using XRD (DMAX2500-PC, Rigaku), high-resolution transmission electron microscopy (HRTEM, FEI F20, operating at 200 kV), and energy-dispersive spectroscopy (EDS, attached to the HRTEM). Ex situ XRD and EXAFS analyses were used to observe the structural changes occurring in the active material of the ZnTe electrode during cycling. The Zn K-edge EXAFS spectra of the ZnTe electrodes were recorded at the 8C (Nano XAFS) beamline on a 3.0 GeV storage ring at the Pohang Light Source (PLS), Korea.

Electrochemical Measurements: For the electrochemical evaluation of Zn, Te, ZnTe, and the ZnTe/C composite, test electrodes consisting of the active powder (70 wt.%), carbon black (Denka, 15 wt.%) as a conducting agent, and polyvinylidene fluoride (PVDF, 15 wt.%) dissolved in N-methyl-2-pyrrolidone (NMP) as a binder were fabricated. Samples of each mixture were vacuum-dried at 120 $^\circ\text{C}$ for 3 h

and pressed (electrode; thickness: ca. 0.045 mm, area: 0.79 cm^2 , weight of active material: ca. 2.5 mg). Coin-type electrochemical cells were assembled in an Ar-filled glove box using a Celgard 2400 separator, Li foil as the counter and reference electrodes, and 1 M LiPF_6 in ethylene carbonate/diethyl carbonate (EC/DEC, 1:1 by volume, Panax

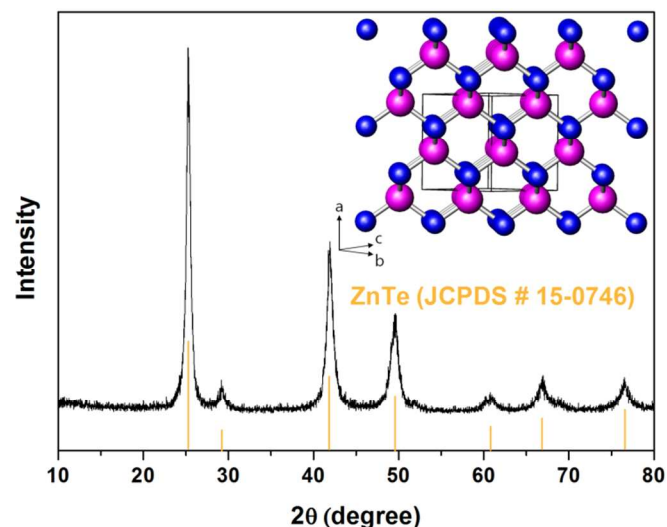


Fig. 1 XRD pattern and crystalline structure of ZnTe.

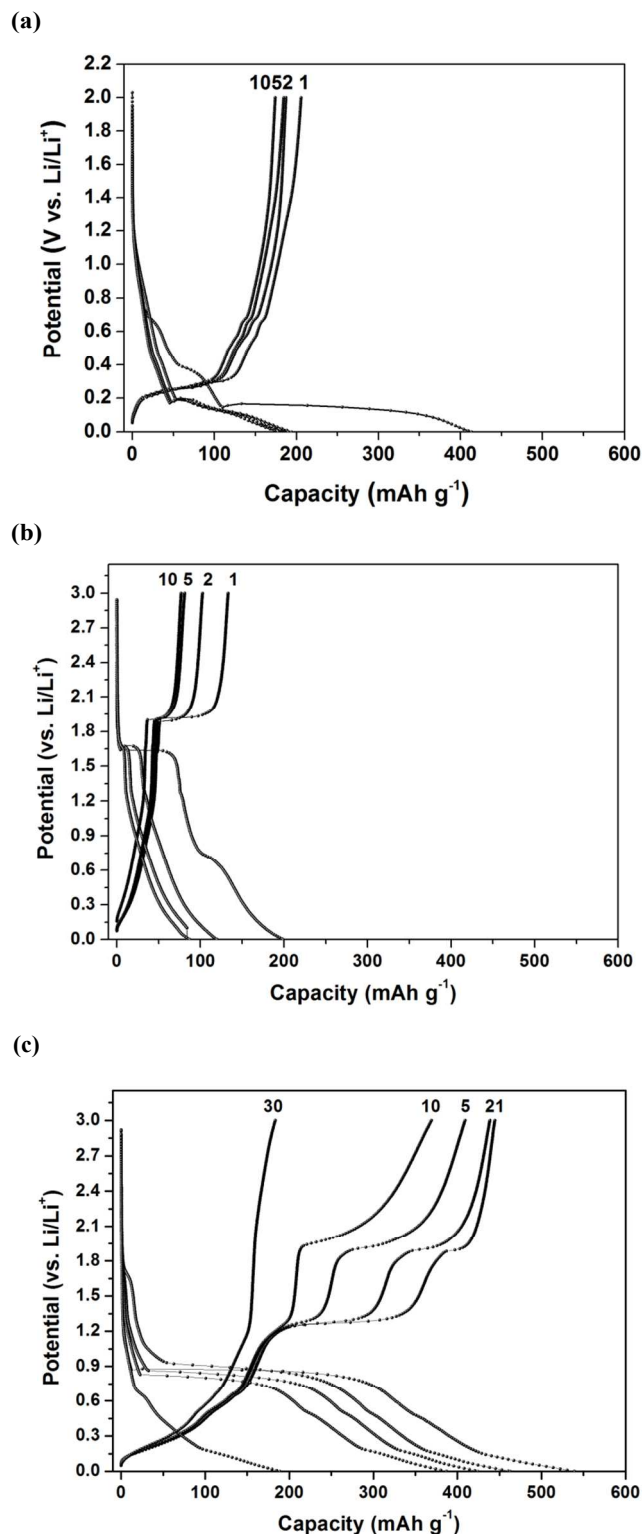


Fig. 2 Voltage profiles of various electrodes: (a) Zn, (b) Te, and (c) ZnTe.

Table 1 First discharge and charge capacities, initial coulombic efficiencies, and capacity retentions of the Zn, Te, and ZnTe electrodes.

Electrode	1st discharge capacity [mAh g ⁻¹]	1st charge capacity [mAh g ⁻¹]	Initial coulombic efficiency [%]	Capacity retention after Xth charge capacity [%]
Zn	413	206	49.9	84.4 (X = 10)
Te	199	133	66.8	57.9 (X = 10)
ZnTe	540	445	82.4	41.1 (X = 30)

STARLYTE) as the electrolyte. CV was measured by SP-240 (Bio-logic) in the range of 0.0–3.0 V at scanning rates of 0.15 mV s⁻¹. All the cells were tested galvanostatically between 0.0 and 3.0 V (vs. Li/Li⁺) at a current density of 100 mA g⁻¹ using a Maccor automated tester. Li is inserted into the working electrode during the discharge reaction and extracted during the charge reaction.

Results and discussion

Fig. 1 shows the XRD pattern and crystalline structure of the

ZnTe sample obtained by a simple HEMM technique. All of the XRD peaks corresponded to the zinc blende ZnTe phase (JCPDS #15-0746) and no other crystalline phases were detected. As shown in the inset in Fig. 1, zinc blende typed ZnTe (JCPDS #15-0746, space group F4-3m, a = 6.102 Å) has an interesting crystalline structure with regard to Li-ion batteries because it contains hexagonal-type channels along the <01-1> direction that facilitate Li diffusion and accommodation.

The voltage profiles of the Zn, Te, and ZnTe electrodes are

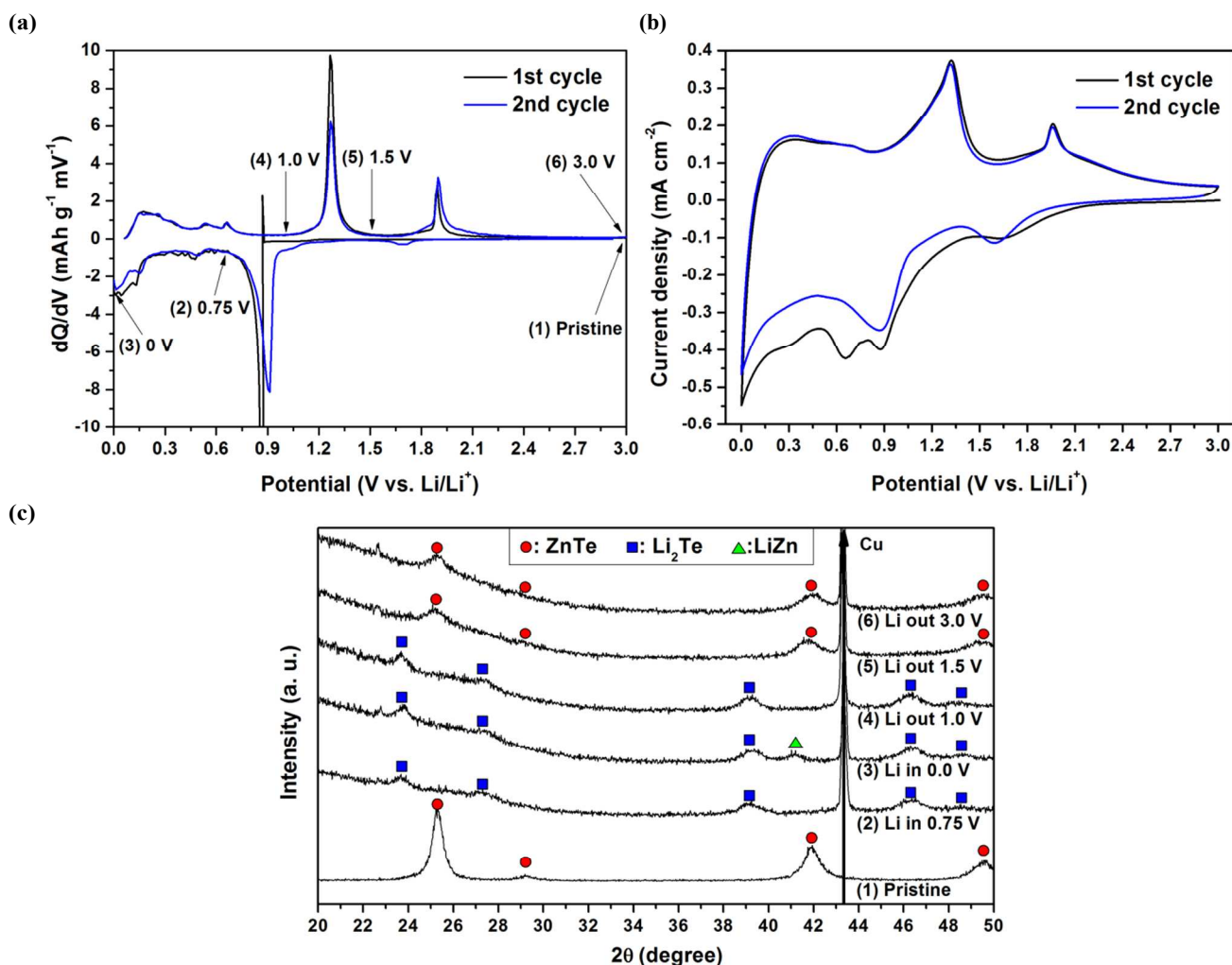


Fig. 3 Electrochemical reaction mechanism between ZnTe and Li: (a) DCP of the first and second cycles, (b) CV of the first and second cycles, and (c) ex situ XRD results of the first cycle for a ZnTe electrode.

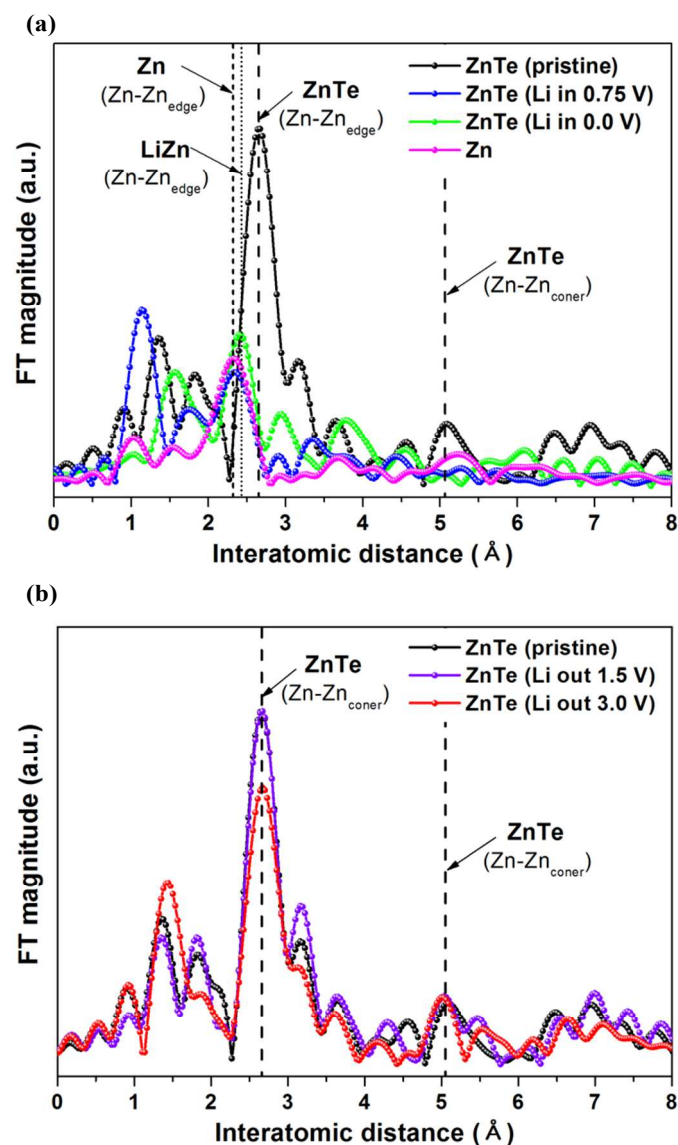


Fig. 4 EXAFS spectra of a ZnTe electrode during the first cycle: (a) first discharge reaction and (b) first charge reaction.

shown in Fig. 2a, b, and c, respectively. The first discharge and

charge capacities alongside the initial coulombic efficiencies and capacity retentions of these electrodes are presented in Table 1. The pure Zn electrode showed poor reversibility with first discharge and charge capacities of 413 and 206 mAh g⁻¹, respectively, and a low initial coulombic efficiency of 49.9% at a current rate of 100 mA g⁻¹. Recently, a study demonstrated that Zn electrode exceeded its theoretical value at equilibrium condition and formed Li_{1.27}Zn corresponding to ca. 520 mAh g⁻¹.⁴² The poor reversibility of the Zn electrode is caused by the large volume change that occurs during the formation of LiZn, and which is associated with the pulverization of the active material and its subsequent electrical isolation.⁴² The pure Te electrode had even poorer discharge and charge capacities; 199 and 133 mAh g⁻¹, with flat discharge and charge potentials of 1.65 V and 1.9 V, respectively. Considering the theoretical capacity (Li₂Te: 420 mAh g⁻¹) of the Te electrode, these small discharge/charge capacities are attributed to the poor electrical conductivity of the Te. Conversely, the ZnTe electrode showed high reversibility with first discharge and charge capacities of 540 and 445 mAh g⁻¹, respectively, and a high coulombic efficiency of 82.4%. Considering the capacity contributed to the formation of solid electrolyte interface (SEI) layer and Li_{1.27}Zn,⁴² it can be concluded that the ZnTe electrode was fully reacted with Li. Although the ZnTe electrode exhibited a better electrochemical performance than the Zn and Te electrodes, its capacity retention after the 30th cycle was only ca. 41.1% of the first charge capacity. The poor capacity retention of the ZnTe electrode may be caused by the large volume change that occurs on the formation of Li₂Te and LiZn phases during the discharge step, followed by pulverization of the active material and its subsequent electrical isolation from the current collector.³⁶⁻⁴²

In Fig. 3a and b, the DCP and CV of the first and second cycles of the ZnTe electrode show several peaks during its discharge and charge reactions. All the peaks of DCP and CV results coincided with each other except a peak of ca. 0.7 V of the first cycle, which corresponded to a reaction potential of SEI layer formation. Ex situ XRD was performed at selected potentials, as indicated by the DCP, and the results are presented in Fig. 3c. When the potential was lowered from open-circuit potential (Fig. 3c-1 to 0.75 V, the ZnTe phase disappeared fully and the Li₂Te phase appeared, as shown in Fig. 3c-2. In the voltage range 0.75 to 0 V, various small peaks appeared in the DCP. The reaction potentials of these peaks were in good agreement with those of various Li_xZn alloy phases such as LiZn₄, Li₂Zn₅, LiZn₂, and Li₂Zn₃.⁴² When the

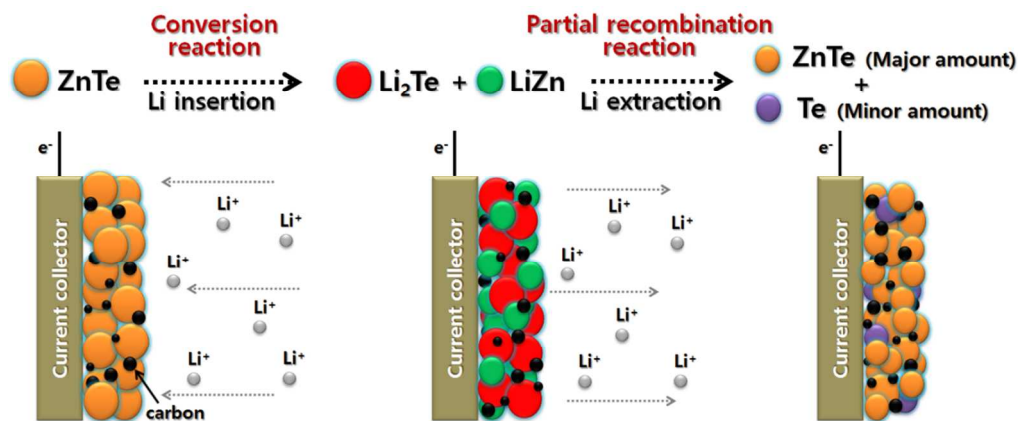


Fig. 5 Schematic diagram of the electrochemical reaction mechanism of a ZnTe electrode during cycling.

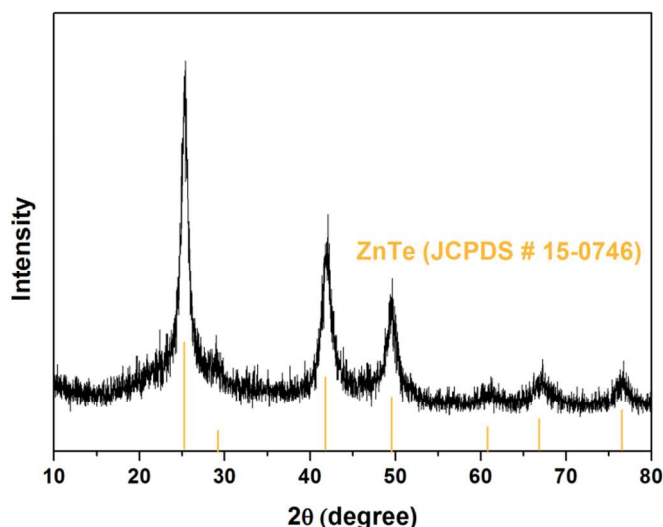


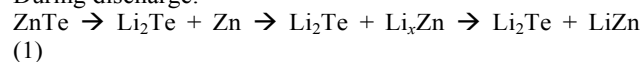
Fig. 6 XRD pattern of the ZnTe/C nanocomposite.

electrode was in its fully discharged state at 0.0 V (Fig. 3c-3), the XRD pattern showed the presence of LiZn and Li₂Te phases, indicating the complete conversion reaction of ZnTe. During the charge step, the LiZn phase disappeared when the potential was increased to 1.0 V (Fig. 3c-4). In the further charged state at 1.5 V (Fig. 3c-5), the Li₂Te phase had transformed into ZnTe. In the fully charged state at 3.0 V (Fig. 3c-6), no additional structural changes were observed, even though a small peak near 1.9 V appeared in the DCP & CV (Fig. 3a and b). A new small peak of 1.65 V during 2nd discharge reaction was appeared. The potentials of 1.9 V during 1st charge and 1.65 V during 2nd discharge reactions were corresponded to the reaction potential of Te electrode as shown in Fig. 2b, which demonstrated that the remaining small amount of Te after recombination of ZnTe was reacted.

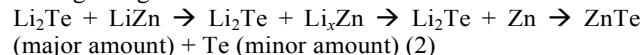
To confirm the proposed reaction mechanism occurring at the ZnTe electrode more accurately, Zn K-edge EXAFS

analysis of the ZnTe electrode was performed and the results are shown in Fig. 4. The main peaks in the EXAFS spectrum of crystalline ZnTe were associated with the Zn-Te (2.64 and 5.06 Å) and Zn-Zn (4.26 Å) bond lengths.⁴⁶ In the discharged state at 0.75 V, the main peak had appeared to 2.33 Å (representing the Zn-Zn interatomic distance in Zn). As shown in Fig. 4a, when the potential was fully discharged at 0 V, the main Zn peak (2.33 Å) had shifted again to 2.42 Å (representing the Zn-Zn interatomic distance in LiZn). In the charged state at 1.5 V, the main EXAFS peaks corresponded to the Zn-Zn_{edge} (2.64 Å) and Zn-Zn_{corner} (5.06 Å) bond lengths of the ZnTe phase (Fig. 4b). This result demonstrates that the ZnTe phase was recombined during the charge step, which is consistent with the ex situ XRD results. This recombination reaction phenomenon is quite interesting and similar to those observed for Sb₂S₃,⁴⁷ SnSb,²⁸ Cu₆Sn₅,⁴⁸ ZnP₂,³⁶ ZnSe,³⁹ ZnSb,^{38,40} and nanosized transition metal oxides³³ and is also supported by the appearance of the same DCP and CV peaks in the 1st and 2nd cycles as shown, previously, in Fig. 3a and b. In the fully charged state at 3.0 V, the EXAFS peaks showed no structural variation, which also demonstrated that the small peak near 1.9 V in the DCP and CV was related to a reaction of Te electrode. On the basis of the above ex situ XRD and EXAFS results, the reactions taking place during the first discharge-charge cycle can be expressed as follows:

During discharge:



During charge:



The ex situ XRD and EXAFS spectra definitely demonstrate that the conversion (1)/partial recombination (2) of the ZnTe electrode during discharge/charge, which is well described

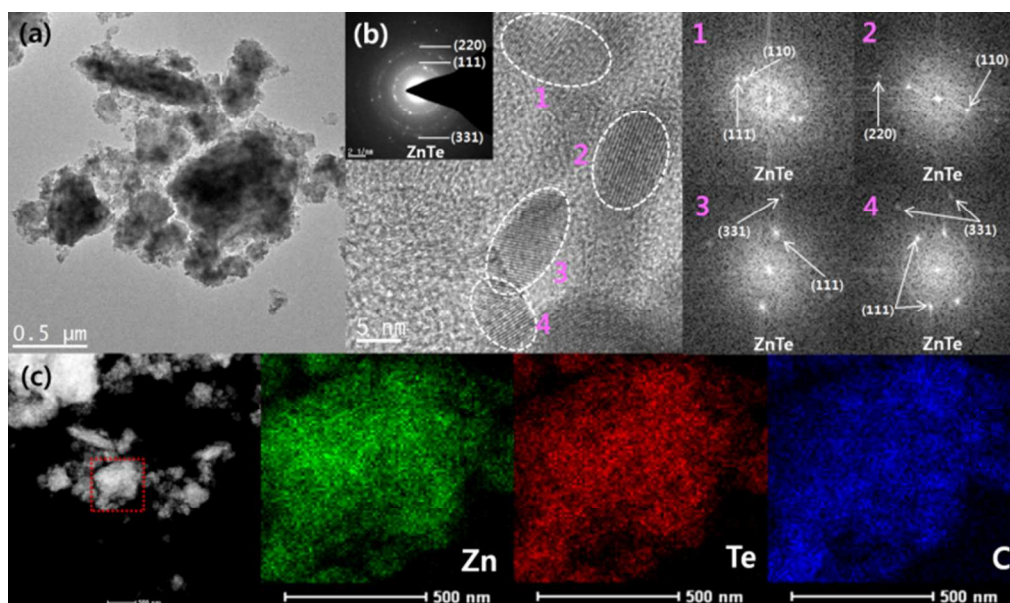


Fig. 7 TEM bright-field image, HRTEM images combined with FT patterns, and STEM image with EDS mapping for the ZnTe/C nanocomposite.

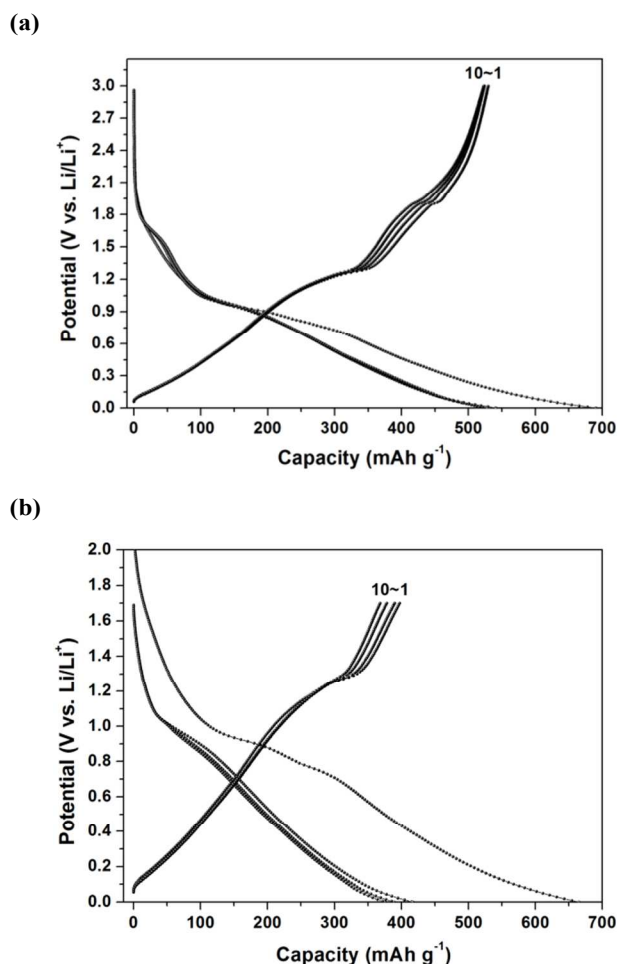


Fig. 8 Voltage profile of a ZnTe/C nanocomposite electrodes: (a) voltage range of 0 to 3.0 V and (b) voltage range of 0 to 1.7 V.

schematically in Fig. 5.

Similar to the S cathode in Li/S batteries or Li-alloy-based

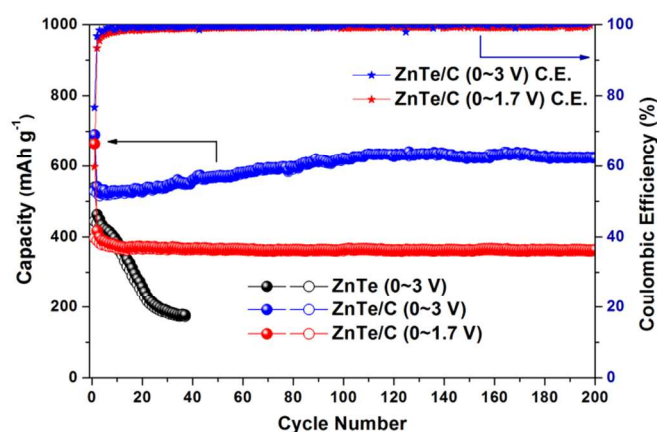


Fig. 9 Comparison of the cycle performances and coulombic efficiencies of pristine ZnTe (voltage range: 0 to 3.0 V) and ZnTe/C nanocomposite electrodes (two voltage ranges: 0 to 1.7 V and 0 to 3.0 V).

anode in Li-ion batteries, nanocomposites modified with carbon produced by HEMM are suitable for fabricating high-performance electrode materials.^{1,24,25,27-30,49-51} This method yields well-distributed, nanosized metal or alloy crystallites within a carbon matrix. HEMM plastically deforms the particles, which leads to work hardening and material fracturing upon impact at temperatures >200 °C and pressures of the order of 6 GPa.⁵² Upon consideration of the HEMM mechanism, a ZnTe/C composite sample was prepared by this method. The XRD pattern of the ZnTe/C composite is shown in Fig. 6. All of the XRD peaks corresponded to ZnTe peaks and no other phases were detected. The average ZnTe nanocrystallite size in the ZnTe/C nanocomposite, estimated using the Scherrer equation, was approximately 8.5 nm.

A TEM bright-field image (Fig. 7a), HRTEM image combined with several Fourier transform (FT) patterns (Fig. 7b), and a STEM image with corresponding energy dispersive X-ray spectroscopy (EDS) mapping (Fig. 7c) for the ZnTe/C nanocomposite are given in Fig. 7. The HRTEM image and FT patterns of the ZnTe/C nanocomposite show that well dispersed ZnTe nanocrystallites with sizes of approximately 5–10 nm were contained within the amorphous carbon matrix, which agrees well with the XRD result. The EDS mapping images also demonstrate that the ZnTe nanocrystallites and amorphous carbon were well dispersed within the composite.

Fig. 8 shows the voltage profiles of the ZnTe/C nanocomposite electrodes. The initial discharge and charge capacities of this electrode within the voltage range of 0 to 3.0 V were 690 and 530 mAh g⁻¹, respectively, with an initial coulombic efficiency of 77% (Fig. 8a). Taking into account the initial irreversible capacities of SEI layer formation and the milled amorphous carbon (corresponding to ca. 392 and 174 mAh g⁻¹ during initial discharge/charge reaction) in the ZnTe/C nanocomposite, the ZnTe in the ZnTe/C nanocomposite electrode almost exhibited complete electrochemical reversibility. Additionally, the electrode showed an initial charge capacity of 400 mAh g⁻¹ within the voltage range of 0 to 1.7 V (Fig. 8b). This high reversibility is attributed to the presence of ZnTe nanocrystallites within the amorphous carbon matrix, which enhance the electrochemical kinetics and electrical conductivity of the composite material. Additionally, their good electrochemical performance can be attributed to the conversion/partial recombination reactions of ZnTe during Li insertion/extraction (Fig. 5). This is because the nanocrystallites

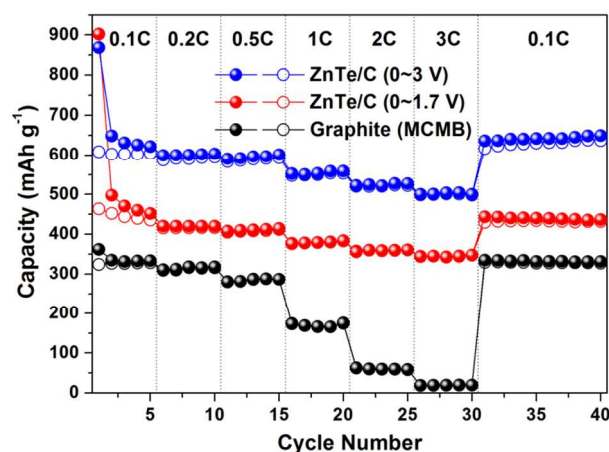


Fig. 10 Comparison of the rate capability of MCMB-graphite and ZnTe/C nanocomposite electrodes.

of binary XY compounds gradually decreased in size to 2-3 nm after a few cycles and then retained this size throughout the subsequent discharge/charge reactions by repeatedly dissociating into Li-X and Li-Y phases and then recombining to form the nanocrystalline binary intermetallic XY phase of within the composite.^{1,53}

The cycle performances of ZnTe and ZnTe/C nanocomposite electrodes are compared at a current rate of 100 mA g⁻¹ in Fig. 9. The cycle performance of the ZnTe electrode was quite poor because of the large volume change that occurred during the formation of the Li₂Te and LiZn phases. The ZnTe/C nanocomposite electrode had a very stable capacity of ca. 623 mAh g⁻¹ over 200 cycles within the 0 to 3.0 V voltage range. Therefore, in this range, the ZnTe/C nanocomposite electrode showed high electrochemical reversibility and stable cycling behavior compared to the ZnTe electrode. On the basis of the proposed reaction mechanism, to avoid reaction of remaining Te and Li, additional cycling behavior in the voltage range of 0 to 1.7 V was observed. In this case, the ZnTe/C nanocomposite electrode also had very stable capacity retention of 91.5% of the initial charge capacity over 200 cycles. These excellent cycle performances were attributed to the uniformly distributed active 5-10 nm ZnTe nanocrystallites, the buffering matrix of amorphous carbon, and the conversion/partial recombination reactions of ZnTe during discharge/charge.

Fig. 10 shows the rate capability of the ZnTe/C nanocomposite (voltage range: 0 to 1.7 V and 0 to 3.0 V) as a function of the C rate, with C being defined as the full use of the restricted charge capacity (600 mAh g⁻¹ (for the voltage range of 0 to 3.0 V) and 450 mAh g⁻¹ (for the voltage range of 0 to 1.7 V) in 1 h. The ZnTe/C nanocomposite electrode showed an excellent rate capability, far better than that of the commercially available MCMB graphite anode. At rates of 1C and 3C, the ZnTe/C nanocomposite electrode (0 to 3.0 V) had very high charge capacities with stable cycling behavior; 553 mAh g⁻¹ and 504 mAh g⁻¹, corresponding to ca. 92% and 84% of the initial charge capacity, for rates of 1C and 3C, respectively. In the voltage range of 0 to 1.7 V, the ZnTe/C nanocomposite electrode also showed good rate capabilities with charge capacities of 380 mAh g⁻¹ and 345 mAh g⁻¹ corresponding to ca. 85% and 77% of the initial charge capacity, for rates of 1C and 3C, respectively. The fast rate capability of the ZnTe/C nanocomposite electrode is attributed to the preparation of well-dispersed 5–10 nm sized nanocrystalline ZnTe within the amorphous carbon matrix by HEMM.

Conclusions

The electrochemical conversion/partial recombination reactions of ZnTe during discharge/charge were demonstrated by conducting ex situ XRD and EXAFS analysis on the basis of the DCP and CV results for the ZnTe electrode. A ZnTe/C nanocomposite, composed of 5-10 nm ZnTe nanocrystallites distributed uniformly within a carbon matrix, was prepared and tested to examine its suitability as an electrode material for rechargeable Li-ion batteries. The ZnTe/C nanocomposite electrode exhibited an excellent electrochemical performance with a high capacity, stable cycling behavior of ca. 623 mAh g⁻¹ over 200 cycles (voltage range: 0 to 3.0 V), and fast rate capability with 92% and 84% retention of the initial charge capacity at rates of 1C and 3C, respectively. ZnTe/C nanocomposites are, therefore, promising materials for improved performance rechargeable Li-ion batteries.

Acknowledgements

This paper was supported by Research Fund, Kumoh National Institute of Technology.

Notes and references

^aSchool of Materials Science and Engineering, Kumoh National Institute of Technology, Gumi, Gyeongbuk 730-701, Republic of Korea. E-mail: cmpark@kumoh.ac.kr; Fax: +82-54-478-7769; Tel: +82-54-478-7746

^bOutstanding Research Group Program, Convergence Technology Research Institute, Kumoh National Institute of Technology, Gumi, Gyeongbuk 730-701, Republic of Korea

† Footnotes should appear here. These might include comments relevant to but not central to the matter under discussion, limited experimental and spectral data, and crystallographic data.

Electronic Supplementary Information (ESI) available: [details of any supplementary information available should be included here]. See DOI: 10.1039/b000000x/

- 1 C.-M. Park, J.-H. Kim, H. Kim, H.-J. Sohn, *Chem. Soc. Rev.*, 2010, **39**, 3115.
- 2 M. Winter, J. O. Besenhard, M. E. Spahr, P. Novak, *Adv. Mater.*, 1998, **10**, 725.
- 3 G.-A. Nazri, G. Pistoia, *Lithium Batteries: Science and Technology*, Kluwer Academic/Plenum, Boston, 2004.
- 4 R. A. Huggins, *Advanced Batteries: Materials Science Aspects*, Springer, New York, 2009.
- 5 D. Aurbach, *Nonaqueous Electrochemistry*, Marcel Dekker, New York, 1999.
- 6 H. Kim, G. Jeong, Y.-U. Kim, J.-H. Kim, C.-M. Park, H.-J. Sohn, *Chem. Soc. Rev.*, 2013, **42**, 9011.
- 7 J. Cabana, L. Monconduit, D. Larcher, M. R. Palacin, *Adv. Energy Mater.*, 2010, **22**, E170.
- 8 P. G. Bruce, B. Scrosati, J.-M. Tarascon, *Angew. Chem. Int. Ed.*, 2008, **47**, 2930.
- 9 N.-S. Choi, Z. Chen, S. A. Freunberger, X. Ji, Y.-K. Sun, K. Amine, G. Yushin, L. F. Nazar, J. Cho, P. G. Bruce, *Angew. Chem. Int. Ed.*, 2012, **51**, 9994.
- 10 R. Marom, S. F. Amalraj, N. Leifer, D. Jacob, D. Aurbach, *J. Mater. Chem.*, 2011, **21**, 9938.
- 11 D. Larcher, S. Beattie, M. Morcrette, K. Edstrom, J.-C. Jumas, J.-M. Tarascon, *J. Mater. Chem.*, 2007, **17**, 3759.
- 12 V. Etacheri, R. Marom, R. Elazari, G. Salitra, D. Aurbach, *Energy & Environ. Sci.*, 2011, **4**, 3243.
- 13 R. A. Huggins, *J. Power Sources*, 1999, **81-82**, 13.
- 14 Y. Idota, T. Kubota, A. Matsufuji, Y. Maekawa, T. Miyasaka, *Science*, 1997, **276**, 1395.
- 15 D. Deng, M. G. Kim, J. Y. Lee, J. Cho, *Energy Environ. Sci.*, 2009, **2**, 818.
- 16 R. Zhang, M. S. Whittingham, *Electrochem. Solid-State Lett.*, 2010, **13**, A184.
- 17 C. J. Wen, R. A. Huggins, *J. Electrochem. Soc.*, 1981, **128**, 1181.
- 18 Y. Yamada, Y. Iriyama, T. Abe, Z. Ogumi, *J. Electrochem. Soc.*, 2010, **157**, A26.
- 19 M. Yoshio, T. Tsumura, N. Dimov, *J. Power Sources*, 2005, **146**, 10.

ARTICLE

- 20 X. Su, Q. Wu, J. Li, X. Xiao, A. Lott, W. Lu, B. W. Sheldon, J. Wu, *Adv. Energy. Mater.*, 2014, **4**, 1300882.
- 21 A. Netz, R. A. Huggins, W. Weppner, *J. Power Sources*, 2003, **119–121**, 95.
- 22 O. Mao, R. A. Dunlap, J. R. Dahn, *J. Electrochem. Soc.*, 1999, **146**, 405.
- 23 D. C. S. Souza, V. Pralong, A. J. Jacobson, L. F. Nazar, *Science*, 2002, **296**, 2012.
- 24 C.-M. Park, H.-J. Sohn, *Adv. Mater.*, 2007, **19**, 2465.
- 25 C.-M. Park, Y.-U. Kim, H.-J. Sohn, *Chem. Mater.*, 2009, **21**, 5566.
- 26 J. Wang, I. D. Raistrick, R. A. Huggins, *J. Electrochem. Soc.*, 1986, **133**, 457.
- 27 C.-M. Park, S. Yoon, S.-I. Lee, J.-H. Kim, J.-H. Jung, H.-J. Sohn, *J. Electrochem. Soc.*, 2007, **154**, A917.
- 28 J.-U. Seo, C.-M. Park, *J. Mater. Chem. A*, 2013, **1**, 15316.
- 29 J. H. Sung, C.-M. Park, *Mater. Lett.*, 2013, **98**, 15.
- 30 J. H. Sung, C.-M. Park, *J. Electroanal. Chem.*, 2013, **700**, 12.
- 31 A. Dailly, J. P. Willmann, D. Billaud, *Electrochim. Acta.*, 2003, **48**, 977.
- 32 A. S. Arico, P. Bruce, B. Scrosati, J.-M. Tarascon, W. V. Schalkwijk, *Nat. Mater.*, 2005, **4**, 366.
- 33 P. Poizot, S. Laruelle, S. Grugeon, L. Dupont, J.-M. Tarascon, *Nature*, 2000, **407**, 496.
- 34 C. K. Chan, H. Peng, G. Liu, K. Meilwrath, X. F. Zhang, R. A. Huggins, Y. Cui, *Nat. Nanotechnol.*, 2008, **3**, 31.
- 35 H. Gleiter, *Prog. Mater. Sci.*, 1989, **33**, 223.
- 36 C.-M. Park, H.-J. Sohn, *Chem. Mater.*, 2008, **20**, 6319.
- 37 M.-P. Bichat, J.-L. Pascal, F. Gillot, F. Favier, *Chem. Mater.*, 2005, **17**, 6761.
- 38 C.-M. Park, H.-J. Sohn, *Adv. Mater.*, 2010, **22**, 47.
- 39 H.-T. Kwon, C.-M. Park, *J. Power Sources*, 2014, **251**, 319.
- 40 M.-G. Park, C. K. Lee, C.-M. Park, *RSC Adv.*, 2014, **4**, 5830.
- 41 Q. Su, Z. Dong, J. Zhang, G. Du, B. Xu, *Nanotechnol.*, 2013, **24**, 255705.
- 42 Y. Hwa, J. H. Sung, B. Wang, C.-M. Park, H.-J. Sohn, *J. Mater. Chem.*, 2012, **22**, 12767.
- 43 R. Amutha, A. Subbarayan, R. Sathyamoorthy, *Cryst. Res. Technol.*, 2006, **41**, 1174.
- 44 N. Amin, K. Sopian, M. Konagai, *Sol. Energy Mater. Sol. Cells*, 2007, **91**, 1202.
- 45 Q. Wu, M. Litz, X. C. Zang, *Appl. Phys. Lett.*, 1996, **68**, 2924.
- 46 S.-W. Han, Y.-D. Choi, *J. Korean Phy. Soc.*, 2008, **53**, 244.
- 47 C.-M. Park, Y. Hwa, N.-E. Sung, H.-J. Sohn, *J. Mater. Chem.*, 2010, **20**, 1097.
- 48 K. D. Kepler, J. T. Vaughey, M. M. Thackeray, *Electrochem. Solid-State Lett.*, 1999, **2**, 307.
- 49 C. Liang, N. J. Dudney, J. Y. Howe, *Chem. Mater.*, 2009, **21**, 4724.
- 50 X. Ji, K. T. Lee, L. F. Nazar, *Nature Mater.*, 2009, **8**, 500.
- 51 A. Manthiram, Y. Fu, Y.-S. Su, *Acc. Chem. Res.*, 2013, **46**, 1125.
- 52 C. Suryanarayana, *Prog. Mater. Sci.*, 2001, **46**, 1.
- 53 C.-M. Park, H.-J. Sohn, *Electrochim. Acta*, 2009, **54**, 6367.